Monthly Notices
of the
ROYAL ASTRONOMICAL SOCIETY

MNRAS **474,** 4730–4739 (2018) doi:10.1093/mnras/stx2957
Advance Access publication 2017 November 21

# The PHEMU15 catalogue and astrometric results of the Jupiter's Galilean satellite mutual occultation and eclipse observations made in 2014–2015

E. Saquet,[1,2]★ N. Emelyanov,[2,3]★ V. Robert,[1,2] J.-E. Arlot,[2] P. Anbazhagan,[4] K. Baillié,[2] J. Bardecker,[5] A. A. Berezhnoy,[3] M. Bretton,[6] F. Campos,[7] L. Capannoli,[8] B. Carry,[2,9] M. Castet,[10] Y. Charbonnier,[11] M. M. Chernikov,[12] A. Christou,[13] F. Colas,[2] J.-F. Coliac,[14] G. Dangl,[15] O. Dechambre,[16] M. Delcroix,[17] A. Dias-Oliveira,[18] C. Drillaud,[19] Y. Duchemin,[2] R. Dunford,[20] P. Dupouy,[21] C. Ellington,[22] P. Fabre,[11] V. A. Filippov,[23] J. Finnegan,[13] S. Foglia,[24] D. Font,[6] B. Gaillard,[10] G. Galli,[24] J. Garlitz,[25] A. Gasmi,[8] H. S. Gaspar,[26] D. Gault,[27] K. Gazeas,[28] T. George,[29] S. Y. Gorda,[30] D. L. Gorshanov,[31] C. Gualdoni,[32] K. Guhl,[33,34] K. Halir,[35] W. Hanna,[36] X. Henry,[11] D. Herald,[37] G. Houdin,[38] Y. Ito,[39] I. S. Izmailov,[31] J. Jacobsen,[40] A. Jones,[41] S. Kamoun,[42] E. Kardasis,[43] A. M. Karimov,[23] M. Y. Khovritchev,[31] A. M. Kulikova,[31] J. Laborde,[21] V. Lainey,[2] M. Lavayssiere,[21] P. Le Guen,[11] A. Leroy,[10] B. Loader,[44] O. C. Lopez,[45,46] A. Y. Lyashenko,[31] P. G. Lyssenko,[23] D. I. Machado,[47,48] N. Maigurova,[49] J. Manek,[50] A. Marchini,[51] T. Midavaine,[52] J. Montier,[53] B. E. Morgado,[18,54] K. N. Naumov,[31] A. Nedelcu,[55] J. Newman,[56] J. M. Ohlert,[57,58] A. Oksanen,[59] H. Pavlov,[60] E. Petrescu,[61] A. Pomazan,[49] M. Popescu,[55] A. Pratt,[62] V. N. Raskhozhev,[12] J.-M. Resch,[11] D. Robilliard,[53] E. Roschina,[31] E. Rothenberg,[34] M. Rottenborn,[63] S. A. Rusov,[31] F. Saby,[11] L. F. Saya,[8] G. Selvakumar,[4] F. Signoret,[64] V. Y. Slesarenko,[31] E. N. Sokov,[31] J. Soldateschi,[51] A. Sonka,[55] G. Soulie,[21] J. Talbot,[65] V. G. Tejfel,[22] W. Thuillot,[2] B. Timerson,[66] R. Toma,[13] S. Torsellini,[8] L.L. Trabuco,[48] P. Traverse,[67] V. Tsamis,[68] M. Unwin,[69] F. Van Den Abbeel,[70] H. Vandenbruaene,[71] R. Vasundhara,[4] Y. I. Velikodsky,[72] A. Vienne,[2,73] J. Vilar,[74] J.-M. Vugnon,[75] N. Wuensche[76] and P. Zeleny[77]

*Affiliations are listed at the end of the paper*

Accepted 2017 November 8. Received 2017 November 3; in original form 2017 August 28

**ABSTRACT**

During the 2014–2015 mutual events season, the Institut de Mécanique Céleste et de Calcul des Éphémérides (IMCCE), Paris, France, and the Sternberg Astronomical Institute (SAI), Moscow, Russia, led an international observation campaign to record ground-based photometric observations of Galilean moon mutual occultations and eclipses. We focused on processing the complete photometric observations data base to compute new accurate astrometric positions. We used our method to derive astrometric positions from the light curves of the events.

★ E-mail: eleonore.saquet@obspm.fr (ES); emelia@sai.msu.ru (NE)

We developed an accurate photometric model of mutual occultations and eclipses, while correcting for the satellite albedos, Hapke's light scattering law, the phase effect, and the limb darkening. We processed 609 light curves, and we compared the observed positions of the satellites with the theoretical positions from IMCCE NOE-5-2010-GAL satellite ephemerides and INPOP13c planetary ephemeris. The standard deviation after fitting the light curve in equatorial positions is ±24 mas, or 75 km at Jupiter. The rms (O−C) in equatorial positions is ±50 mas, or 150 km at Jupiter.

**Key words:** techniques: photometric – astronomical data bases: miscellaneous – eclipses – ephemerides – occultations – planets and satellites: general.

## 1 INTRODUCTION

The Jovian system and the Galilean moons have been studied for their motion, in particular. Their respective dynamical models allow us to constrain their structure and their origin theories (Lainey, Duriez & Vienne 2004a; Lainey et al. 2009; Lainey, Arlot & Vienne 2004b).

Photometric observations of mutual events of the Galilean moons are essential to improve their ephemerides, mainly because we are able to extract highly precise astrometric positions of the satellites from the photometry. The precision of the mutual event observations is up to 20 mas for the Galilean moons (Arlot et al. 2014), or 60 km at the distance of Jupiter. Moreover, Robert et al. (2017) have recently demonstrated, for the inner satellites of Jupiter, that the positional accuracy derived from photometric observations still remains more precise than that derived from direct astrometry, even if the use of the most recent *Gaia*-DR1 catalogue (Gaia Collaboration et al. 2016) allowed them to eliminate the systematic errors due to the star references. Thus, our work is crucial for current and future spacecraft navigation (Dirkx et al. 2016), and for dynamical purposes, since the ephemerides are improved by adjusting the new astrometric positions to the theories.

In 2014–2015, the Institut de Mécanique Céleste et de Calcul des Éphémérides (IMCCE) and the Sternberg Astronomical Institute (SAI) organized a worldwide observation campaign to record a maximum of mutual occultations and eclipses of the Galilean moons. In this paper, we present the results of this campaign, with the photometric and astrometric data.

## 2 THE MUTUAL EVENTS

When the common Galilean orbital plane crosses the ecliptic plane, mutual events can occur. Depending on the configuration from the Earth or the Sun, we will speak about occultations or eclipses. Occultations can occur when the Joviocentric declination of the Earth becomes zero, whereas eclipses can occur when the Joviocentric declination of the Sun becomes zero.

The 2014–2015 period was very favourable since 442 events were observable from 2014 September 1 to 2015 July 20. To compute the predictions of all the 2014–2015 events, we used the IMCCE NOE-5-2010-GAL satellite ephemerides (Lainey et al. 2009) and INPOP13c planetary ephemeris (Fienga et al. 2014). The NOE numerical code is a gravitational *N*-body code that incorporates highly sensitive modelling and can generate partial derivatives needed to fit initial positions, velocities, and other parameters (like the ratio $k_2/Q$) to the observational data. The code includes (i) gravitational interaction up to degree two in the spherical harmonics expansion of the gravitational potential for the satellites and up to degree six for Jupiter (Anderson et al. 1996, 1998, 2001a,b; Jacobson 2001); (ii) the perturbations of the Sun (including inner planets and the Moon by introducing their mass in the Solar one) and Saturn using DE430 ephemerides; (iii) the Jovian precession; and (iv) the tidal effects introduced by means of the Love number $k_2$ and the quality factor $Q$. The dynamical equations are numerically integrated in a Jovicentric frame with inertial axes (conveniently the Earth mean equator J2000). The equation of motion for a satellite $P_i$ is detailed in Lainey, Dehant & Pätzold (2007).

**Table 1.** Raw statistics of the PHEMU85, PHEMU91, PHEMU97, PHEMU03, PHEMU09, and PHEMU15 campaigns.

| | 1985 | 1991 | 1997 | 2003 | 2009 | 2015 |
|---|---|---|---|---|---|---|
| Observation sites | 28 | 56 | 42 | 42 | 74 | 75 |
| Light curves | 166 | 374 | 292 | 377 | 457 | 609 |
| Observable events | 248 | 221 | 390 | 360 | 237 | 442 |
| Observed events | 64 | 111 | 148 | 118 | 172 | 236 |
| Observed/observable events | 0.26 | 0.50 | 0.38 | 0.33 | 0.72 | 0.53 |

By comparison, only 237 events were observable in 2009 and 360 in 2003. The results of the previous observation campaign can be found in Arlot et al. (2014). In Table 1, we show the raw statistics of the PHEMU85 (Arlot et al. 1992), PHEMU91 (Arlot et al. 1997), PHEMU97 (Arlot et al. 2006), PHEMU03 (Arlot et al. 2009), PHEMU09 (Arlot et al. 2014), and PHEMU15 campaigns. We observe a constant increase in the numbers of the observation sites, of the light curves, and of the observed events. This denotes the increase in the interest of the non-professional community in these campaigns.

We have already demonstrated, during the previous campaigns, that photometric records of mutual events are accurate enough for astrometric purposes, and that our method provides a high positional accuracy (Arlot et al. 2014). More recently, Robert et al. (2017) have demonstrated that the positional accuracy derived from photometry of mutual events still remains more precise than that derived from direct astrometry for the inner satellites of Jupiter.

## 3 THE PHEMU15 CAMPAIGN

### 3.1 Report

Following the previous mutual event campaign successes, we organized PHEMU15, an international observation campaign to record as many events as possible. To fill in an eventual lack of data due to poor weather, we encouraged observers in different countries to acquire events, and to observe the same events from various longitudes.

During this campaign, we observed 236 events and a same event was recorded 17 times. We received 643 light curves, and astrometric results were calculated for 609 of them. Thirty-four light curves

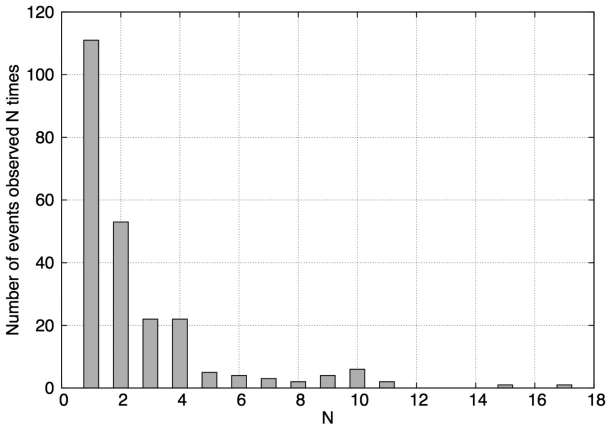


**Figure 1.** Raw statistics of the number of events observed $N$ times.

could not be used for several reasons such as a non-event detection, an observation after the minimum, or an observation of an occultation and an eclipse at the same time. Fig. 1 shows the raw statistics of the observed events and numbers of corresponding observations.

We distinguished the source of data within two categories. Source I gathered the photometric observations made by the IMCCE observation team. Records were obtained at Pic du Midi Observatory (IAU code 586) and Haute-Provence Observatory (IAU code 511). We extracted the satellite flux for 35 events to produce the light curves before treatment. Then, Source A gathered other observations made by professional or non-professional observers around the world. The satellite flux was directly extracted by the observers who transmitted their light curves to the IMCCE for treatment.

### 3.2 Observation sites

75 observation sites were involved in the 2014–2015 campaign. For several sites, more than one telescope was used to record events. We have introduced a special code to identify each observation facility. A correspondence between the facility and their conventional code is given in the data base[1] with the astrometric results in electronic form at the Natural Satellites DataBase (NSDB) service of IMCCE. Table 2 shows raw statistics of the different observation sites of the campaign. Starting from the left-hand column, we provide the number of observations received $O$, the number of observations $R$ for which astrometric results were calculated, the number of observations $N$ for which the light curves showed no events, the number of observations $S$ for which an occultation and an eclipse occurred at the same time, the location of the observer, and, if relevant, their IAU code. In the very few cases when an occultation and an eclipse occurred at the same time, we could not provide astrometric results. We plan to take into account such events in future improvements.

## 4 LIGHT-CURVE REDUCTION

### 4.1 Photometric reduction

Mutual events can be recorded with a video camera that provides a movie, or a CCD camera that provides FITS images (Pence et al. 2010). In both cases, we need the most accurate timing, that is to say, better than 0.1 s. Note that the satellite Io, for example, has a velocity of 17.2 km s$^{-1}$, so that an accuracy of 0.1 s of time corresponds to an accuracy of 1.7 km in space. An accuracy better than 0.1 s of time is necessary, since the internal accuracy of the motion theory of the satellites is around 1 km (Lainey, private communication). Most of the time, aperture photometry is applied for the light flux extraction. This technique consists of summing the illuminated pixels of a satellite, and subtracting the contribution from the sky background. Many events were recorded with at least two satellites in the camera field, the occulted or eclipsed satellite, and one to three reference satellites. At least, one reference satellite is needed to minimize an eventual flux inconsistency due to the atmospheric extinction.

For each event, we created a file containing metadata in the head lines, and following lines containing the UTC date, the measured flux (or magnitude) for the satellites involved in the event, and the flux (or magnitude) for the reference satellites. These files are provided in the IMCCE data base as well.

Figs 2–6 show light-curve examples and corresponding model adjustments. Figs 4 and 5, in particular, show one event recorded by two different observers. The longer integrating time for each point in Fig. 5 gives a signal less noisy than in Fig. 4.

### 4.2 Astrometric reduction

Positional and astrometric data were determined from the measurements of satellite fluxes during their mutual occultations or eclipses, using the procedure described in Emelianov (2003), and in Emelyanov & Gilbert (2006). We used an $S$ value that traduces the normalized flux emitted by the observed satellites during an event. $S = 1$ before and after the event, and $S < 1$ during the mutual occultation or eclipse.

Given the topocentric distances of the satellites, we considered the projections $X(t)$ and $Y(t)$ of the angular separation between the satellites on to the celestial parallel and meridian, respectively. $S$ can be written as a function $S(X(t), Y(t))$.

We define $E_i$ the observed photometric flux at time $t_i$ ($i = 1, 2, \ldots, m$). $m$ is the number of photometric counts during a single event. With chosen planet and satellite theories of motion, one can compute for each time $t_i$ the theoretical values of functions $X(t)$, $Y(t)$, i.e. $X_{\rm th}(t_i)$, $Y_{\rm th}(t_i)$. The calculated values of $X(t_i)$, $Y(t_i)$ differ from $X_{\rm th}(t_i)$, $Y_{\rm th}(t_i)$ by constant corrections $D_x$, $D_y$, i.e.

$$\begin{cases} X(t) = X^{\rm th}(t) + D_x \\ Y(t) = Y^{\rm th}(t) + D_y. \end{cases}$$

Our method consists of solving conditional equations

$$E_i = K\, S(X_{\rm th}(t_i) + D_x,\, Y_{\rm th}(t_i) + D_y) \qquad (i = 1, 2, \ldots, m)$$

for constants $D_x$, $D_y$, and K.

We linearize conditional equations with respect to parameters $D_x$, $D_y$, and then solve the system using the least squares method. This means 'fitting the light curve'.

The astrometric result of the reduction of a single event photometric observation is written by

$$\begin{cases} X = X(t^*) = X_{\rm th}(t^*) + D_x \\ Y = Y(t^*) = Y_{\rm th}(t^*) + D_y, \end{cases}$$

where $t^*$ is an arbitrary time instant inside the event interval. Actually, we assume that it is the time instant for which $\sqrt{X^2 + Y^2}$ reaches its minimum value, i.e. $t^*$ is the time of the closest apparent approach of the satellites.

[1] Full explanation table is available in electronic form at the NSDB service of IMCCE via http://nsdb.imcce.fr/obspos/phemuAR/explan2_e.htm

**Table 2.** Observation sites for the PHEMU15 campaign. We provide the number of observations received *O*, the number of observations *R* for which astrometric results were calculated, the number of observations *N* for which the light curves showed no events, the number of observations *S* for which an occultation and an eclipse occurred at the same time and for which the astrometric results could not be obtained, the location of the observer, and, if relevant, their IAU code.

| *O* | *R* | *N* | *S* | Site, country | IAU code |
|---|---|---|---|---|---|
| Source I | | | | | |
| 11 | 10 | 1 | 0 | Haute-Provence Obs., France | 511 |
| 24 | 21 | 3 | 0 | Pic du Midi Obs., France | 586 |
| Source A | | | | | |
| 48 | 47 | 1 | 0 | Desert Springs, Australia | |
| 3 | 3 | 0 | 0 | Umatilla, USA | |
| 41 | 41 | 0 | 0 | Scottsdale, USA | |
| 10 | 10 | 0 | 0 | Kuriwa Obs., Australia | E28 |
| 9 | 7 | 0 | 2 | Tunis, Tunisia | |
| 16 | 15 | 0 | 1 | La Couyere Astro. Center, France | J23 |
| 36 | 35 | 1 | 0 | Murrumbateman, Austrialia | E07 |
| 14 | 14 | 0 | 0 | Puig d'Agulles, Spain | |
| 8 | 8 | 0 | 0 | Tangra Obs., Australia | E24 |
| 5 | 5 | 0 | 0 | Elgin, USA | |
| 5 | 5 | 0 | 0 | Toulon, France | |
| 10 | 10 | 0 | 0 | Kourovskaya, Russia | 168 |
| 8 | 8 | 0 | 0 | Chaneyville, USA | |
| 16 | 12 | 4 | 0 | Mundolsheim, France | |
| 5 | 5 | 0 | 0 | Cogolin, France | |
| 18 | 17 | 0 | 1 | West Park Obs., England | Z92 |
| 5 | 5 | 0 | 0 | Itajuba, Brazil | 874 |
| 5 | 5 | 0 | 0 | Iguacu, Brazil | X57 |
| 2 | 2 | 0 | 0 | Como, Italy | C13 |
| 1 | 1 | 0 | 0 | Arnold, USA | |
| 3 | 3 | 0 | 0 | Vesqueville, Belgique | 231 |
| 11 | 11 | 0 | 0 | Newark, USA | H95 |
| 2 | 1 | 1 | 0 | Baronnies Provencales Obs., France | B10 |
| 7 | 7 | 0 | 0 | Waikanae, New Zealand | |
| 1 | 1 | 0 | 0 | Kingman, USA | |
| 5 | 4 | 1 | 0 | Marseille, France | |
| 6 | 6 | 0 | 0 | Tielt, Belgium | |
| 2 | 2 | 0 | 0 | Dax Obs., France | 958 |
| 2 | 2 | 0 | 0 | Hyères, France | |
| 3 | 3 | 0 | 0 | Siena, Italy | K54 |
| 6 | 4 | 1 | 1 | Trebur, Germany | 239 |
| 1 | 1 | 0 | 0 | Gardnerville, USA | |
| 9 | 9 | 0 | 0 | Montigny-le-Bretonneux, France | |
| 2 | 2 | 0 | 0 | Malemort-du-Comtat, France | |
| 4 | 3 | 1 | 0 | Darfield, New Zealand | |
| 2 | 2 | 0 | 0 | Gretz-Armainvilliers, France | A07 |
| 4 | 4 | 0 | 0 | Cabudare, Venezuela | |
| 2 | 2 | 0 | 0 | Nikolaev, Ukraine | 089 |
| 1 | 1 | 0 | 0 | La Grimaudière, France | |
| 6 | 3 | 3 | 0 | Flynn, Australia | |
| 7 | 7 | 0 | 0 | Egeskov Obs., Danemark | |
| 4 | 3 | 1 | 0 | Salvia Obs., France | I73 |
| 11 | 11 | 0 | 0 | Biesenthal, Germany | |
| 2 | 2 | 0 | 0 | Maidenhead, England | I64 |
| 6 | 6 | 0 | 0 | Oberkrämer, Germany | |
| 1 | 1 | 0 | 0 | Comthurey, Germany | |
| 6 | 6 | 0 | 0 | Rokycany Obs., Czech Republic | K61 |
| 6 | 6 | 0 | 0 | Archenhold-Obs., Germany | |
| 1 | 1 | 0 | 0 | Slovice, Czech Republic | |
| 1 | 1 | 0 | 0 | Fouras, France | |
| 24 | 24 | 0 | 0 | Vainu Bappu Obs., India | 220 |
| 13 | 12 | 1 | 0 | Horice, Czech Republic | |
| 14 | 13 | 1 | 0 | Alma-Ata, Kazakhstan | 210 |
| 1 | 1 | 0 | 0 | Antibes, France | 139 |
| 12 | 11 | 1 | 0 | Sendai, Japan | 391 |
| 13 | 13 | 0 | 0 | Nonndorf, Austria | C47 |

**Table 2** – *continued*

| *O* | *R* | *N* | *S* | Site, country | IAU code |
|---|---|---|---|---|---|
| 6 | 6 | 0 | 0 | GiaGa Obs., Italy | 203 |
| 1 | 1 | 0 | 0 | Saulges, France | I73 |
| 1 | 1 | 0 | 0 | Waianae Beach, New Zealand | |
| 2 | 0 | 0 | 2 | Dienville, France | |
| 2 | 2 | 0 | 0 | Gassin, France | |
| 1 | 1 | 0 | 0 | Le Mesnil-Saint-Denis, France | |
| 44 | 44 | 0 | 0 | Pulkovo Obs., Russia | 084 |
| 2 | 2 | 0 | 0 | Naperville, USA | W08 |
| 7 | 7 | 0 | 0 | Pulkovo-Kislovodsk, Russia | C20 |
| 4 | 4 | 0 | 0 | Voronezh, Russia | |
| 17 | 16 | 1 | 0 | Bucharest, Romania | 073 |
| 6 | 6 | 0 | 0 | Laval, Canada | 818 |
| 28 | 23 | 3 | 2 | Armagh Obs., Northern Ireland | 981 |
| 4 | 4 | 0 | 0 | Athens, Greece | 066 |
| 2 | 2 | 0 | 0 | Nyrola Obs., Finland | 174 |
| 12 | 12 | 0 | 0 | Praha, Czech Republic | |
| 3 | 3 | 0 | 0 | Tournefeuille, France | |
| 643 | 609 | 34 | 9 | TOTAL | |

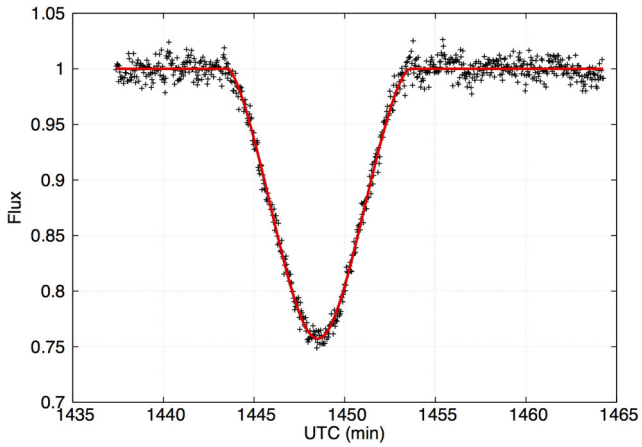


**Figure 2.** Europa occults Io on 2015 January 6. The dots denote observational data, and the line denotes the model adjustment. The light curve is perfectly modelled and the observation is not noisy.

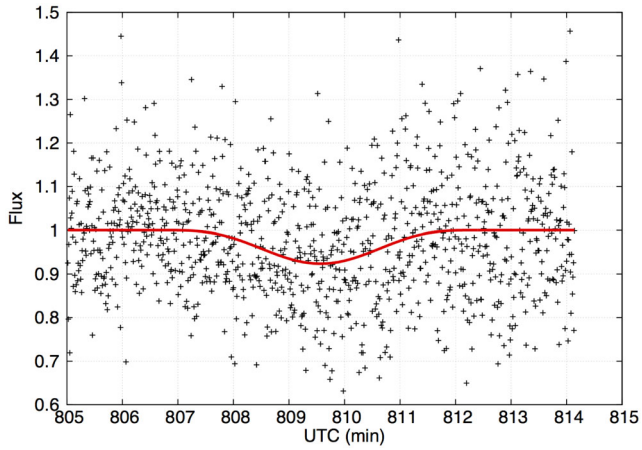


**Figure 3.** Io eclipses Ganymede on 2015 January 22. The dots denote observational data, and the line denotes the model adjustment. This observation shows a grazing event with a small magnitude drop. The signal is noisy and could be improved with a longer integrating time for each point.

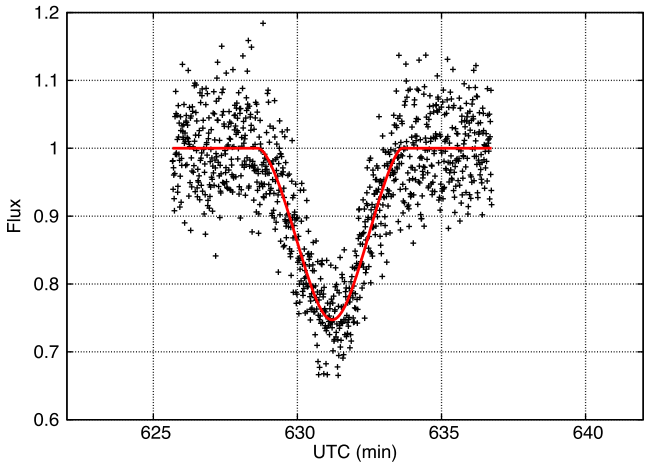


**Figure 4.** Europa occults Io on 2015 March 22. The dots denote observational data, and the line denotes the model adjustment. The observation is noisy.

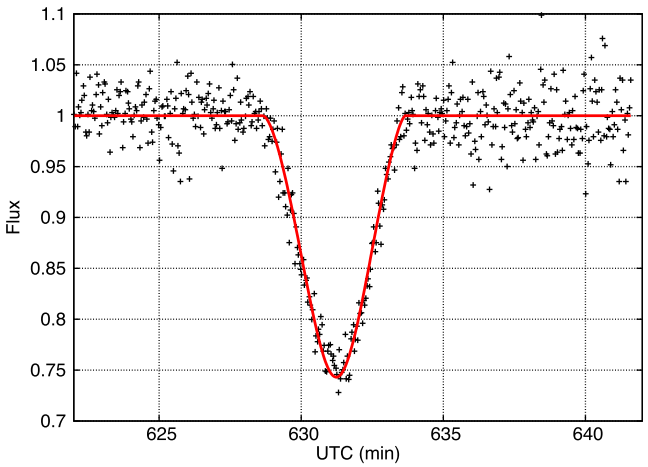


**Figure 5.** Europa occults Io on 2015 March 22. The dots denote observational data, and the line denotes the model adjustment. This is the same event as in Fig. 4, but the integration time was different.

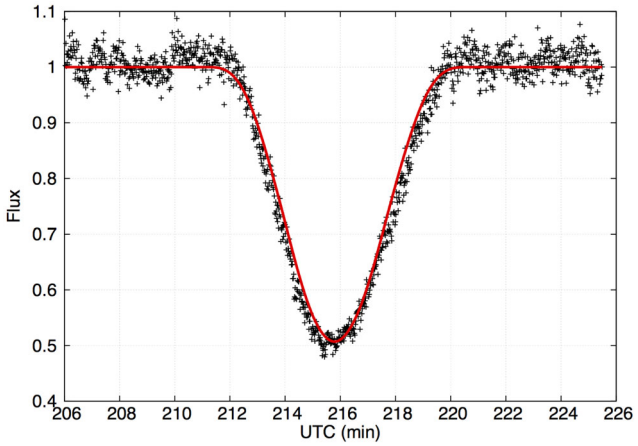


**Figure 6.** Io eclipses Ganymede on 2015 February 27. The dots denote observational data, and the line denotes the model adjustment. This is a full eclipse.

Astrometric results are provided as intersatellite tangential $(X, Y)$ coordinates in equatorial positions, where $X = \Delta\alpha\cos\delta$ and $Y = \Delta\delta$ at the instant of the satellites' closest approach $t^*$. $\Delta\alpha$ and $\Delta\delta$ are the position differences in right ascension and declination, respectively, given in the 'occulting minus occulted' or 'eclipsing minus eclipsed' directions. We provide astrometric results in an ICRS topocentric frame in the case of mutual occultations, and in an ICRS heliocentric frame in the case of mutual eclipses. Note that in the case of full events, i.e. a total occultation or eclipse, only the position angle $P$ can be determined. The position angle is defined as

$$\tan P = \frac{Y}{X}.$$

In our solution, we used the IMCCE NOE-5-2010-GAL satellite ephemerides. The JUP310 ephemerides (Jacobson 2013) can also be used. Both ephemerides use the PHEMU85, PHEMU91, PHEMU97, and PHEMU03 mutual events data set for their construction, with astrometric observations data set which differs between JPL (Jacobson 2013) and NOE (Lainey et al. 2009).

## 5 THE RESULTING DATA BASES

### 5.1 Photometric result data base

The observation files are available in electronic form at the NSDB service of IMCCE. We composed a catalogue that consists of 609 files, corresponding to the observations for which astrometric results were calculated. For each line of the files, we provide the metadata of the mutual events, then the UTC observation time, the photometric measurements of the event, and if recorded, the photometric measurements of the reference satellites.

### 5.2 Astrometric result data base

The astrometric results are divided in two sections. The first section is related to the events for which the tangential $(X, Y)$ coordinates could be computed, and the second is related to the full events for which only the position angle $P$ could be computed. In this section, the apparent relative position of the satellite measured across the apparent trajectory cannot be fixed definitively, and therefore position angles can be determined only up to $\pm 180^\circ$.

Table 3 gives an extract of the astrometric results of the first section. Starting from the left-hand column, we provide the observatory code, the event type, the UTC date, the tangential $(X(t^*), Y(t^*))$ coordinates in equatorial positions, the standard deviation after fitting the light curve characterizing the accuracy of the photometry estimated via the least-squares method, the (O−C) computed from the NOE-5-2010-GAL satellite ephemerides characterizing the agreement between theory and observations, the angular separation $s$, the position angle $P$, an estimation of the results quality and reliability $Q$, and the normalized flux minimum level $F_{\rm min}$. The observatory code identifies not only the observatory but also the instrument used, and the precise site coordinates: The longitude and latitude coordinates are given with a $10^{-6^\circ}$ precision, and the altitude coordinate is given with a $10^{-1}$ m precision. Details are given in the explanation text accompanying the astrometric results in NSBD data base. In the event type column, $N_{\rm a}{\rm o}N_{\rm p}$ denotes an occultation with the active (occulting) satellite number $N_{\rm a}$ and the passive (occulted) satellite number $N_{\rm p}$. $N_{\rm a}{\rm e}N_{\rm p}$ denotes an eclipse with the active (eclipsing) satellite number $N_{\rm a}$ and the passive (eclipsed) satellite number $N_{\rm p}$, as well. The angular separation is defined as

$$s = \sqrt{X^2 + Y^2}.$$

The estimation of the results quality and reliability $Q$ are as follows:

(i) 1 for the doubtful results as divergent results for a same event, or a large shift in the time moment, or low-quality photometry.
(ii) 0 for the non-doubtful results.

Table 4 gives an extract of the astrometric results of the second section. Starting from the left-hand column, we provide the observatory code, the event type, the UTC date, the position angle $P$, the standard deviation after fitting the light curve, and the (O−C) of the apparent relative satellite position along the satellite track computed from the NOE-5-2010-GAL satellite ephemerides. Examples of modelling are shown in Figs 2–6, as red lines.

## 6 ACCURACY OF THE ASTROMETRIC RESULTS

We compared the positions of the Galilean satellites with their theoretical computed positions given by the NOE-5-2010-GAL and JUP310 satellite ephemerides. The distributions of the (O−C) in tangential coordinates and the corresponding standard deviation after fitting the light curve are provided in Fig. 7 and Table 5 for the NOE-5-2010-GAL satellite ephemerides. They show the difference (RA, Dec.) coordinates for individual satellites. Table 6 provides the (O−C) distribution for the JUP310 satellite ephemerides.

We used $Q = 0$ as an indicator to define the best observations in our set. This concerns 511 observations. Offsets for this observation set are −1.8 and 0.1 mas in right ascension and declination, respectively, according to NOE-5-2010-GAL. They are negligible and we may deduce that some mismodelling of photometric corrections remains. Offsets according to JUP310 are slightly higher: 1.5 mas in right ascension and −8.9 mas in declination.

The key point is that the NOE-5-2010-GAL mean rms (O−C) between right ascension and declination for all these observations is 49.9 mas. This mean rms (O−C) between right ascension and declination corresponds to our observation accuracy. The JUP310 average rms (O−C) for all these observations is 65.5 mas. We observe a difference of 15 mas between both ephemerides, or 45 km at Jupiter, which is consistent since NOE-5-2010-GAL and JUP310

MNRAS 474, 4730–4739 (2018)

**Table 3.** Extract of the astrometric results for which the tangential coordinates in equatorial positions could be computed. The full table is available in electronic form at the Natural Satellites DataBase service of IMCCE via http://nsdb.imcce.fr/obsphe/obsphe-en/fjuphemu.html.

| Observatory code | Type | Date (YYYY MM DD) | UTC (h m s) | $X(t^*)$ (arcsec) | $Y(t^*)$ (arcsec) | $\sigma_X$ (arcsec) | $\sigma_Y$ (arcsec) | O − C$_X$ (arcsec) | O − C$_Y$ (arcsec) | $s$ (arcsec) | $P$ (°) | $Q$ | $F_{\min}$ |
|---|---|---|---|---|---|---|---|---|---|---|---|---|---|
| ADS | 4e3 | 2014 09 11 | 20 57 26.40 | −0.2945 | −0.1747 | 0.0120 | 0.0358 | − 0.0239 | 0.0022 | 0.3424 | 239.325 | 0 | 0.3619 |
| KIS | 3e4 | 2014 10 07 | 00 08 47.00 | 0.0523 | 0.1717 | 0.0025 | 0.0039 | − 0.0108 | 0.0913 | 0.1795 | 16.950 | 0 | 0.1113 |
| KIS | 2o3 | 2014 10 21 | 02 03 26.25 | −0.2812 | −0.7463 | 0.0274 | 0.0122 | 0.1930 | 0.1211 | 0.7976 | 200.642 | 1 | 0.9532 |
| | | | – | | | | | | | | | | |
| ADS | 1o2 | 2014 11 19 | 18 14 32.65 | −0.1432 | −0.3692 | 0.0431 | 0.0363 | 0.3751 | − 0.0387 | 0.3960 | 201.197 | 1 | 0.7462 |
| KUR | 3o1 | 2014 11 22 | 16 34 56.93 | −0.0954 | −0.2483 | 0.0089 | 0.0164 | − 0.1058 | − 0.2080 | 0.2660 | 201.019 | 1 | 0.6050 |
| ADS | 1o3 | 2014 11 26 | 18 37 19.13 | 0.0962 | 0.2484 | 0.0188 | 0.0204 | 0.0427 | 0.0757 | 0.2664 | 21.168 | 0 | 0.7013 |
| KIS | 3o1 | 2014 12 06 | 22 15 7.88 | 0.1542 | 0.4006 | 0.0050 | 0.0049 | 0.0172 | 0.1056 | 0.4292 | 21.047 | 0 | 0.6603 |
| ALM | 2e3 | 2014 12 09 | 22 43 4.58 | −0.2622 | −0.7572 | 0.0137 | 0.0079 | 0.0289 | 0.0707 | 0.8013 | 199.098 | 0 | 0.9395 |
| ARO | 2o1 | 2014 12 12 | 23 43 8.80 | −0.1194 | −0.4123 | 0.0071 | 0.0088 | − 0.0022 | − 0.0071 | 0.4292 | 196.145 | 0 | 0.6104 |
| | | | – | | | | | | | | | | |
| PIC | 2e1 | 2015 01 06 | 22 33 28.04 | −0.2167 | −0.6007 | 0.0030 | 0.0016 | 0.0086 | − 0.0136 | 0.6386 | 199.839 | 0 | 0.8647 |
| OHP | 2e1 | 2015 01 06 | 22 33 27.10 | −0.2221 | −0.6153 | 0.0046 | 0.0024 | 0.0014 | − 0.0275 | 0.6542 | 199.846 | 0 | 0.8778 |
| OHP | 2o1 | 2015 01 07 | 00 08 38.21 | 0.1540 | 0.3869 | 0.0016 | 0.0015 | − 0.0012 | − 0.0167 | 0.4164 | 21.705 | 0 | 0.7584 |
| OHP | 2o1 | 2015 01 07 | 00 08 20.36 | 0.1611 | 0.4046 | 0.0099 | 0.0094 | − 0.0463 | 0.0218 | 0.4355 | 21.705 | 0 | 0.7690 |
| PIC | 2o1 | 2015 01 07 | 00 08 38.78 | 0.1532 | 0.3847 | 0.0017 | 0.0015 | − 0.0005 | − 0.0195 | 0.4141 | 21.707 | 0 | 0.7572 |
| PIC | 2o1 | 2015 01 07 | 00 08 38.53 | 0.1524 | 0.3828 | 0.0051 | 0.0046 | − 0.0020 | − 0.0211 | 0.4120 | 21.704 | 0 | 0.7561 |
| | | | – | | | | | | | | | | |
| MUR | 1e2 | 2015 06 13 | 08 51 46.45 | 0.2086 | 0.5111 | 0.0069 | 0.0047 | − 0.0115 | − 0.0088 | 0.5520 | 22.200 | 0 | 0.7138 |
| KUR | 1e2 | 2015 06 13 | 08 51 44.75 | 0.2104 | 0.5153 | 0.0070 | 0.0046 | − 0.0175 | − 0.0015 | 0.5566 | 22.208 | 0 | 0.7199 |
| FLY | 1e2 | 2015 06 13 | 08 51 57.88 | 0.1724 | 0.4226 | 0.0119 | 0.0088 | 0.0049 | − 0.1188 | 0.4564 | 22.191 | 0 | 0.8138 |
| CAC | 1e2 | 2015 06 16 | 22 01 31.55 | 0.2055 | 0.5024 | 0.0126 | 0.0088 | − 0.0162 | − 0.0260 | 0.5428 | 22.246 | 0 | 0.7014 |
| UMA | 2o1 | 2015 06 26 | 04 53 47.33 | 0.0969 | 0.2535 | 0.0083 | 0.0073 | − 0.0211 | − 0.0199 | 0.2714 | 20.918 | 0 | 0.7423 |

**Table 4.** Extract of the astrometric results for which only the position angle could be computed. The full table is available in electronic form at the Natural Satellites DataBase service of IMCCE via http://nsdb.imcce.fr/obsphe/obsphe-en/fjuphemu.html.

| Observatory code | Type | Date (Y M D) | UTC (h m s) | $P$ (°) | $\sigma$ (arcsec) | O-C (arcsec) |
|---|---|---|---|---|---|---|
| VBO | 2o4 | 2014 11 27 | 22 08 52.26 | 200.934 | 0.0044 | 0.0164 |
| AAT | 3o1 | 2014 11 29 | 19 23 51.85 | 21.076 | 0.0111 | 0.0510 |
| ADS | 3o1 | 2014 12 14 | 18 49 25.02 | 20.128 | 0.0027 | 0.0059 |
| ALM | 3o1 | 2014 12 14 | 21 31 13.25 | 22.385 | 0.0015 | 0.0336 |
| | | – | | | | |
| ELG | 2e1 | 2015 02 22 | 02 45 15.28 | 200.622 | 0.0091 | 0.0223 |
| ADS | 2o1 | 2015 02 25 | 15 10 05.34 | 19.706 | 0.0035 | 0.0268 |
| SEN | 2o1 | 2015 02 25 | 15 10 10.26 | 19.640 | 0.0040 | 0.0538 |
| VBO | 2o1 | 2015 02 25 | 15 10 04.58 | 199.669 | 0.0018 | 0.0207 |
| KOU | 2e1 | 2015 02 25 | 15 55 10.32 | 20.606 | 0.0032 | 0.0194 |

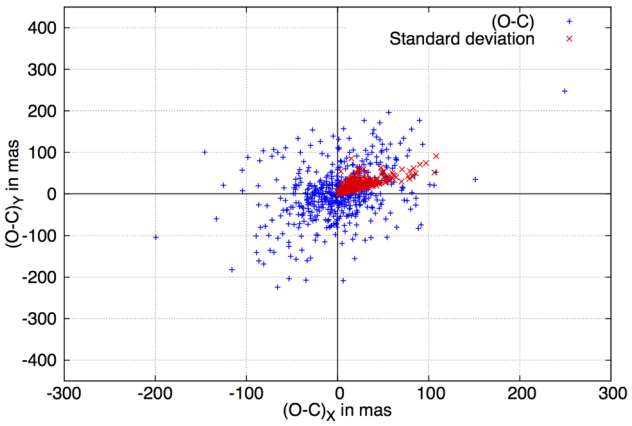


**Figure 7.** Equatorial (O−C) shows the differences between the observed satellite positions (light curve) and its theoretical positions according to NOE-5-2010-GAL ephemerides, for the observation set $Q = 0$ (blue crosses). Red crosses denote the standard deviation $\sigma_X$ and $\sigma_Y$, after fitting the light curve that shows the random errors of photometry.

**Table 5.** Quality characteristics of the derived astrometric positions in mas, according to NOE-5-2010-GAL ephemerides for the best observations ($Q = 0$). $\overline{(O-C)}$ means the mean value of the $(O-C)_X$ and $(O-C)_Y$ deviations.

| | $X(t^*)$ | $Y(t^*)$ |
|---|---|---|
| $\overline{(O-C)}$ | −1.8 | 0.1 |
| rms (O−C) | 39.2 | 60.7 |
| Standard deviations $\sigma_X$, $\sigma_Y$ after fitting the light curve | 23.6 | 24.6 |

**Table 6.** Quality characteristics of the derived astrometric positions in mas, according to JUP310 ephemerides for the best observations ($Q = 0$). $\overline{(O-C)}$ means the mean value of the $(O-C)_X$ and $(O-C)_Y$ deviations.

| | $X(t^*)$ | $Y(t^*)$ |
|---|---|---|
| $\overline{(O-C)}$ | 1.5 | −8.9 |
| rms (O−C) | 51.8 | 78.8 |

satellites ephemerides use almost the same data set for their construction.

## 7 CONCLUSIONS

The IMCCE and SAI organized the 2014–2015 PHEMU15 international observation campaign of the mutual events of the Galilean satellites. All the photometric observations of mutual occultations and eclipses were reduced. 609 astrometric results were calculated.

The standard deviations after fitting the light curve in equatorial positions are 23.6 and 24.6 mas in right ascension and declination, respectively. The rms (O−C) in equatorial positions are ±39.2 and ±60.7 mas in right ascension and declination, respectively, according to NOE-5-2010-GAL satellite ephemerides. These results are better than those of the previous PHEMU09 campaign, and confirm the high value in observing mutual events.

The next campaign will begin in 2021 January and end in 2021 November. The occurrence will be less favourable since the maximum of events will occur at the conjunction of Jupiter with the Sun, and 192 events will be observable. The 2021 campaign will be more favourable to the Southern hemisphere, due to Jupiter's declination.

## ACKNOWLEDGEMENTS

This work was supported by the Russian Foundation for Basic Research, project No. 16-52-150005-CNRS-a. The research work of A. A. Berezhnoy was financially supported by Research Program No. 7 of the Presidium of the Russian Academy of Science. Thirty-five mutual events were recorded at the 1-m telescope of Pic du Midi Observatory (S2P) and at the 80-cm and the 1m20 telescopes of the Haute-Provence Observatory.

## REFERENCES

Anderson J. D., Lau E. L., Sjogren W. L., Schubert G., Moore W. B., 1996, Nature, 384, 541

Anderson J. D., Schubert G., Jacobson R. A., Lau E. L., Moore W. B., Sjogren W. L., 1998, Science, 281, 2019

Anderson R. C., Dohm J. M., Golombek M. P., Haldemann A. F. C., Franklin B. J., Tanaka K. L., Lias J., Peer B., 2001a, J. Geophys. Res., 106, 20563

Anderson J. D., Jacobson R. A., McElrath T. P., Moore W. B., Schubert G., Thomas P. C., 2001b, Icarus, 153, 157

Arlot J. E. et al., 1992, A&AS, 92, 151
Arlot J. E. et al., 1997, A&AS, 125, 399
Arlot J.-E. et al., 2006, A&A, 451, 733
Arlot J.-E. et al., 2009, A&A, 493, 1171
Arlot J.-E. et al., 2014, A&A, 572, A120
Dirkx D., Lainey V., Gurvits L. I., Visser P. N. A. M., 2016, Planet. Space Sci., 134, 82
Emelianov N. V., 2003, Sol. Sys. Res., 37, 314
Emelyanov N. V., Gilbert R., 2006, A&A, 453, 1141
Fienga A., Manche H., Laskar J., Gastineau M., Verna A., 2014, in INPOP new release: INPOP13c. IMCCE, Observatoire de Paris, Paris
Gaia Collaboration et al., 2016, A&A, 595, A2
Jacobson R. A., 2001, AAS/Division for Planetary Sciences Meeting Abstracts #33. p. 1039
Jacobson R., 2013, JUP 310 Release, available at: http://naif.jpl.nasa.gov/pub/naif/JUNO/kernels/spk/jup310.bsp.lbl
Lainey V., Duriez L., Vienne A., 2004a, A&A, 420, 1171
Lainey V., Arlot J. E., Vienne A., 2004b, A&A, 427, 371
Lainey V., Dehant V., Pätzold M., 2007, A&A, 465, 1075
Lainey V., Arlot J.-E., Karatekin Ö., van Hoolst T., 2009, Nature, 459, 957
Pence W. D., Chiappetti L., Page C. G., Shaw R. A., Stobie E., 2010, A&A, 524, A42
Robert V., Saquet E., Colas F., Arlot J.-E., 2017, MNRAS, 467, 694

[1]*Institut Polytechnique des Sciences Avancées IPSA, 63 bis Boulevard de Brandebourg, F-94200 Ivry-sur-Seine, France*
[2]*IMCCE, Observatoire de Paris, PSL Research University, CNRS-UMR 8028, Sorbonne Universités, UPMC, Univ. Lille 1, 77 Av. Denfert-Rochereau, F-75014 Paris, France*
[3]*M. V. Lomonosov Moscow State University – Sternberg astronomical institute, 13 Universitetskij prospect, 119992 Moscow, Russia*
[4]*Vainu Bappu Observatory, Indian Institute of Astrophysics, Bangalore, Karnataka 560034, India*
[5]*International Occultation Timing Association (IOTA), North America and RECON, Gardnerville, NV 89410, USA*
[6]*Observatoire des Baronnies Provencales, 05150 Moydans, France*
[7]*Puig d'Agulles, Spain*
[8]*High-school Liceo G.Galilei, 53100 Siena, Italy*
[9]*Université Côte d'Azur, Observatoire de la Côte d'Azur, CNRS, Lagrange, 06108 Nice cedex 2, France*
[10]*Association T60, Observatoire Midi Pyrénées 14 Avenue Edouard Belin, F-31000 Toulouse, France*
[11]*Observatoire du Pic des Fees, 26 bis allee des pinsons, F-83400 Hyeres, France*
[12]*Voronezh State University, Voronezh 394036, Russia*
[13]*Armagh Observatory and Planetarium, College Hill, Armagh, BT61 9DG, UK*
[14]*Association Andromède Observatoire de Marseille, 13004 Marseille, France*
[15]*Nonndorf 12, 3830, Austria*
[16]*Club Eclipse, 20 rue Jean Monnet, F-78180 Montigny Le Bretonneux, France*
[17]*Société Astronomique de France, commission des observations planétaires, 2, rue de l'Ardèche, F-31170 Tournefeuille, France*
[18]*Observatório Nacional MCTI, rua Gal. J. Cristino 77, Rio de Janeiro, RJ, 20921-400, Brazil*
[19]*Club Eclipse, 1 rue des Peupliers, F-92190 Meudon, France*
[20]*Naperville, near Chicago, IL 60540, USA*
[21]*Observatoire de Dax, rue Pascal Lafitte, F-40100 Dax, France*
[22]*International Occultation Timing Association (IOTA), PO Box 7152, Kent, WA 98042, USA*
[23]*Fessenkov Astrophysical Institute, Alma-Ata 050056, Kazakhstan*
[24]*GiaGa Observatory, Via Mozart 4, I-20010 Pogliano Milanese, Italy*
[25]*American Association of Variable Star Observers (AAVSO), Elgin, Oregon, USA*
[26]*UNESP Campus de Guaratinguet, Av. Ariberto Pereira da Cunha 333, Guaratinguet 12516-410, Brazil*
[27]*Kuriwa Observatory, 22 Booker Road Hawkesbury Heights, NSW 2777, Australia*
[28]*Department of Astrophysics, Astronomy and Mechanics, University of Athens, University Campus, 15784 Zografos, Athens, Greece*
[29]*International Occultation Timing Association (IOTA), Scottsdale, AZ 85255, USA*
[30]*Kourovskaya observatory of the Ural Federal University, Prospect Lenina 51, 620000 Ecaterinbourg, Russia*
[31]*Central Astronomical Observatory of the Russian Academy of Sciences at Pulkovo 196140, Russia*
[32]*Societá Astronomica Ticinese (CH), 6605 Locarno, Italy*
[33]*International Occultation Timing Association (IOTA), European Section, Barthold-Knauststr. 8, D-30459 Hannover, Germany*
[34]*Archenhold-Observatory, Alt-Treptow 1, D-12435 Berlin, Germany*
[35]*Rokycany Observatory, Rokycany 337 01, Czech Republic*
[36]*Royal Astronomical Society of New Zealand, Occultation Section; International Occultation Timing Association (IOTA), Desert Springs, NT 0870, Australia*
[37]*3 Lupin Pl, Murrumbateman, NSW 2582, Australia*
[38]*Club d'astronomie d'Antony, 92160 Antony, France*
[39]*6-2-69-403 Kamisugi, Aoba-ku, Sendai, Miyagi 980-0011, Japan*
[40]*Egeskov Observatory, Syrenvej 6, 7000 Fredericia, Denmark*
[41]*Maidenhead SL6 1XE, UK*
[42]*Société Astronomique de Tunisie, Tunis*
[43]*Hellenic Amateur Astronomy Association, GR-16121 Athens, Greece*
[44]*Royal Astronomical Society of New Zealand, Occultation Section, International Occultation Timing Association, 14 Craigieburn Street, 7510 Darfield, New Zealand*
[45]*Andres Bello Astronomical Complex, 3023 Cabudare, Venezuela*
[46]*Venezuelan Society of Amateur Astronomers, Caracas, Miranda 1074, Venezuela*
[47]*Universidade Estadual do Oeste do Paran a (Unioeste), Avenda Tarqu nio Joslin dos Santos 1300, Foz do Iguau, Brazil*
[48]*Polo Astronmico Casimiro Montenegro Filho/FPTI-BR, Avenida Tancredo Neves 6731, Foz do Iguau, Brazil*
[49]*Research Institute Nikolaev Astronomical Observatory, 54000, Ukraine*
[50]*Czech Astronomical Society - Occultation Section, Observatory Rokycany, Werichova 950/9, CZ-152 00 Praha 5, Czech Republic*
[51]*Astronomical Observatory, Department of Physical Sciences, Earth and Environment, University of Siena, 53100, Italy*
[52]*Club Eclipse, Salvia Observatory, 53100, Mayenne 53, France*
[53]*Société d'Astronomie de Rennes, F-35000 Rennes, France*
[54]*Observatório do Valongo/UFRJ, Ladeira Pedro Antonio 43, Rio de Janeiro 20080-090, Brazil*
[55]*The Astronomical Institute of the Romanian Academy, Bucharest Observatory, Str. Cutitul de Argint 5, 040557 Bucuresti, Romania*
[56]*Canberra Astronomical Society, Australia*
[57]*University of Applied Sciences, D-61169 Friedberg, Germany*
[58]*Astronomie Stiftung Trebur, D-65468 Trebur, Germany*
[59]*Nyrola Observatory, Vertaalantie 449, 41140 Nyrölä, Finland*
[60]*Tangra Observatory, 9 Chad Pl, St Clair, NSW 2759, Australia*
[61]*Amiral Vasile Urseanu Observatory, 010671, Bucharest, Romania*
[62]*International Occultation Timing Association (IOTA), IOTA-ES, West Park Observatory, LS16 Leeds, England*
[63]*Valcha E2671, Plzeň, Czech Republic*
[64]*Groupement Astronomique Populaire de la Région d'Antibes, 2, Rue Marcel-Paul, F-06160 Juan-Les-Pins, Antibes, France*
[65]*Wellington Astronomical Society, 3 Hughes St, 5036 Waikanae Beach, New Zealand*
[66]*International Occultation Timing Association (IOTA), Newark, NY 07104, USA*
[67]*Association Club Eclipse et club Albiréo78, Le Mesnil, F-78320 Saint Denis Yvelines, France*
[68]*Laval, Quebec, Canada*
[69]*Dunedin Astronimical Society, Royal Astronomical Society of New Zealand*
[70]*Observatoire de Vesqueville, 6870 Vesqueville, Belgium*

[71] *Kasteelstraat 224, Tielt, Belgium*
[72] *National Aviation University, 02000 Kiev, Ukraine*
[73] *Université Lille 1, Impasse de l'Observatoire, F-59000 Lille, France*
[74] *SAF groupe Alsace, 8 rue des ormes, F-67450 Mundolsheim, France*
[75] *Club Eclipse, 22 rue du Borrego – BAL149, F-75020 Paris, France*
[76] *International Occultation Timing Association, European Section (IOTA-ES), Bahnhofstrasse 117, D-16359 Biesenthal, Germany*
[77] *Pod Lipou 1532, Hořice, Czech Republic*

This paper has been typeset from a TEX/LATEX file prepared by the author.